NO_X REDUCTION FROM CI ENGINES WITH DC CORONA DISCHARGE - AN EXPERIMENTAL STUDY.

Jan Vinogradov, Eran Sher, Boris Rivin
The Pearlstone Center for Aeronautical Studies, the Department of Mechanical Engineering,
Ben-Gurion University of the Negev, Beer-Sheva, Israel.
jan@bgumail.bgu.ac.il

ABSTRACT

An experimental study of DC corona discharge technology for NO_x reduction from diesel engine exhaust is presented. The DC corona reactor consists of a flat electrode against a multi-needle electrode.

The results are presented in terms of the cleanness (the mass of removed NO_x referred to its initial mass), and the energy consumption (the mass of NO_x per unity corona electric energy). For both cleanness and energy consumption, negative polarity (negative needles) is preferable. The cleanness was found to be independent of the engine load. The results show that the performance of a DC corona reactor depends on the reactor length, electrodes' separation distance, and needle's density. The effectiveness of the NO_x decomposition was mapped, and optimal geometrical parameters for the best reactor performance have been obtained.

It is concluded that for best performance, the residence time of the exhaust gas inside the reactor should be longer than 1.2 seconds; the electrodes' separation distance must be less than 30mm (in order for the electric field intensity to remain sufficiently high for dissociation reactions); and the needles separation distance must not exceed 20mm (in order to provide sufficiently dense distribution of plasma regions from each needle). The cleanness and energy consumption values for the optimal geometry lay between 55%, 17.2gr-NOx/kW-h, and 46%, 27gr-NOx/kW-h for needles separation distance of 10 and 20mm, respectively.

INTRODUCTION

In response to public pressure, controlling hazardous substances from being emitted into the ambient environment has become a major focus of the scientific community. One of the major pollutants is NO_x, known for its perilous effects on human health and environment**.** The term NO_x denotes nitric oxides NO and NO_2, which are produced in combustion process due to high temperatures inside the combustion chamber. These oxides cause eye, throat, and lung irritation and produced mainly by motor vehicles [1].

In last two decades the possibility of NO_x reduction from exhaust gases ($DeNO_x$ process) by means of electric discharge has been intensively studied [2,3]. It has been revealed that chemically active radicals produced in the ionized gaseous media interact with pollutant molecules, converting them to non hazardous substances. Keeping in mind that the Diesel exhaust gas contains water vapor, oxygen, CO_2, nitrogen, and traces of pollutants, the ionization processes in it, resulting in radicals' production, is similar to the one taking place in humid air.

The ionization initiates when free electrons, accelerated by electric field, collide with neutral species. The source for free electrons may be either naturally produced electrons from cosmic radiation, or electron emitter, like one used in electron beam devices. Cosmic radiation produces electrons at a rate of ~1 el/mm^3s. This leads to rather low background electron densities of 10^3-10^6 el/cm^3. This can imply that it takes some time for an electron to be at the right place, i.e. a region where the electric field is high enough. This time is called *inception time lag* and in practice it varies from about 1 ns to many microseconds [4]. The

electron-molecule collisions can result in molecule excitation or its ionization, as well as they can be absolutely elastic and then, only kinetic energy is transmitted. Since average molecule is thousands times heavier than electron, the mean velocity, which molecule gains from elastic collision with the electron, due to energy exchange with it, is comparable to its thermal velocity. In case of ionized molecule, at atmospheric pressure, where the concentration of neutral species is high and therefore ion's mean free path (m.f.p.) is short, ionized species' velocity at the end of its m.f.p. is also low. Thus, in either case, both ionized and neutral species remain slow or cold in sense of their velocity, and this charge transform is referred to as cold plasma. In cold plasma the ionization of one molecule by collision with another can be neglected.

By using an asymmetric electrode pair a non-uniform electric field is produced. Free electrons, which are present in the interelectrode space, are accelerated by electric field towards anode. Field enhancement near one electrode is required. The most common methods used in practice for this purpose are point-to-plane and wire-in-cylinder geometries. In order for an electron to accumulate sufficient energy along its m.f.p. for collisional ionization of neutral species, the electric field intensity should be higher than 24.4kV/cm [5]. At these conditions additional electrons are produced from the collision, and the so-called electron avalanche is initiated. For electric field higher than 24.4kV/cm ionization processes prevail over electron attachment, and therefore the total ionization coefficient α^*, which is defined as a subtraction between first ionization coefficient of Townsend α and attachment coefficient η, becomes positive. Within the interelectrode space, defined as ionization layer, in which the electric field is higher than 24.4kV/cm, recombination of electrons with positive ions is negligible [6]. Beyond the ionization boundary, attachment prevails over ionization and the number of electrons decreases with the decrease of electric field. Thus, only ions transfer the charge, and the interelectrode space beyond the ionization layer is referred to as drift region.

EXPERIMENTAL SETUP

Experimental investigation of CI engine exhaust treatment was made on Mitsubishi 3 cylinder diesel with total volume of 1300cc. The engine was mounted on a test bench and connected to a 3-phase generator, which provides the engine loading, when connected to external heaters. The heaters are capable of consuming a total amount of electric power up to 8kW, taken from 10kW of maximal engine power. The engine speed is kept constant and equal to 1500rpm, in order to maintain standard 50Hz AC supplied to the heaters.

A flow rate of 8L/min from approximately 1000L/min was set to pass through the DC reactor. High voltage supplier, capable of delivering maximum 50kV DC corona voltage is connected to the reactor. The limiting resistor of 6MΩ was connected in series, and the total current and voltage were measured. Thus, controlled by the current, the potential difference on the reactor can be easily calculated. The scheme of the experimental setup is shown in Fig.1. A luminescent type gas analyzer Sun-DGA1000 is connected to the exhaust pipe downstream the reactor. A thermocouple is installed at the entry to the reactor, in order to provide simultaneous temperature measurement**.**

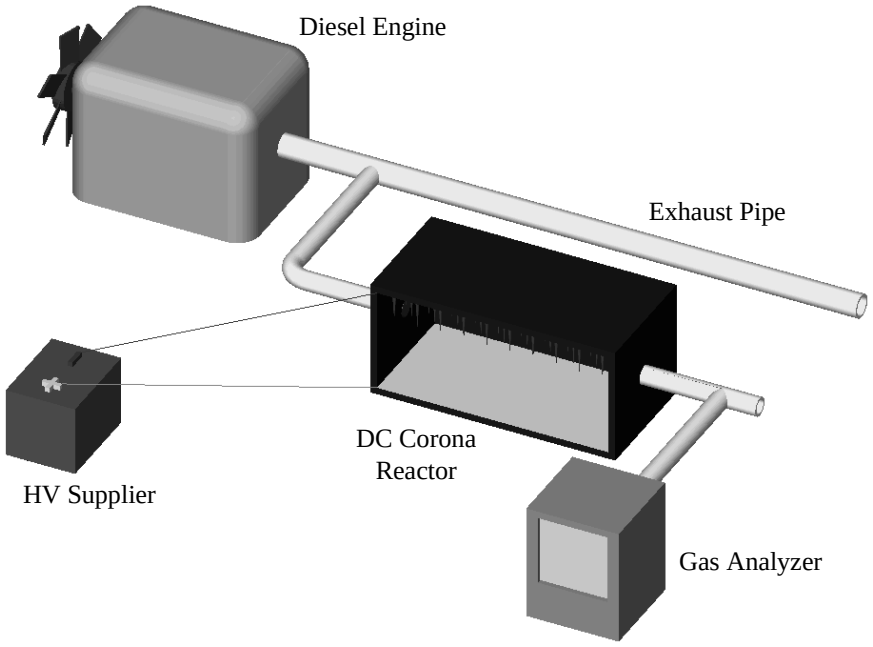

Fig. 1: Experimental setup.

The reactor is built as a box that has a rectangular cross section with 100 x 100 mm inner dimensions. The box is made of Perspex and has an adjustable horizontal plate capable of moving upwards and downwards inside the reactor. Standard medical needles of 0.6 mm external diameter are installed to the plate, connected to each other and to the outgoing electric wire, defining one of the two electrodes. The needles are arranged in staggered rows, separated by ***a*.** At the bottom of the reactor, stainless steel plate with length and width equal to the inner box dimensions is placed. The lower plate is connected to the second outgoing wire, defining the electrode of opposite polarity. A sketch of the corona reactor is shown in Fig.2.

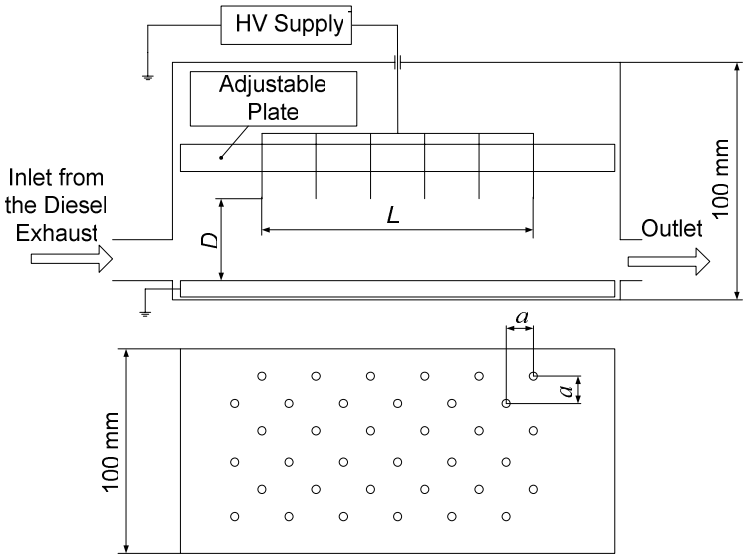

Fig.2: DC corona reactor sketch.

Experiments were carried out for eight typical values of *D* (14, 20, 25, 30, 35, 40, 45, and 50mm), which denotes the distance between the needles' tips and the flat electrode. The

number of rows that defines the multi-needle electrode length *L* was changed from 45 to 150mm. The separation distance between the rows of the needles *a* was set at four different values: 5, 10, 15, and 20mm. Electric voltage has been gradually increased and NO_x, O_2, CO, CO_2, UHB concentrations, voltage and current have been recorded at different polarities and engine loads.

RESULTS AND DISCUSSION

The length and relatively high thermal conductivity of the connection between the exhaust pipe of the engine and the reactor box, allows achieving constant bulk temperature of approximately 25^{o}C inside the reactor, regardless of the engine load.

In this work NO_x *cleanness* is defined as the mass of removed NO_x relative to its initial mass, and NO_x removal *energy consumption* as a mass of removed NO_x per unit corona energy.

The experimental results show that polarity of corona discharge has significant effect on both the cleanness and the energy consumption. In order to understand this phenomenon, a comparison of Voltage Current Characteristics (VCC) for both polarities is made. As it is shown in Fig.3, the total current obtained for positive corona (positive potential on the needles) is higher initially than the one of the negative corona, but at higher voltage the negative ion current overshoots the positive one. It is shown experimentally that the total current is independent of *a*, i.e. the ionization from the single needle is not affected by neighbor needles. Thus, the current for specific value of *D* from several needles can be simply divided by their number and compared to analytical calculation [7, 8], in which only one needle is considered.

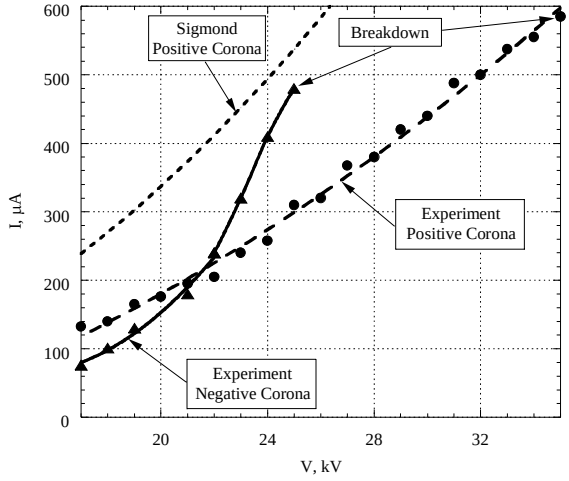

Fig. 3: VCC experimental VS VCC calculated by Sigmond [7] for *D*=30mm, *a*=10mm, *L*=50mm.

The Sigmond's saturation current [7] presented in Fig.3 is higher than both the negative and the positive corona currents, measured experimentally. From Sigmond's model it follows that if the measured current is lower than the saturation one, then for both polarities there are only ions of the same positive or negative charge produce current flow outside the ionization layer, i.e. unipolar corona takes place. Since the current obtained for negative corona lies beneath the saturation current for positive corona, there are no free electrons in the drift region [7].

The lower value of negative corona current at low voltage follows from the higher average mobility of positive ions, which are mainly presented by N_2^+. The main ions,

participating in charge transfer in negative corona are O_2^-, OH^-, and CO_2^-, their mobility is much lower compared to N_2^+. With increase of voltage the electric field intensity increases, and the positive ions that approach cathode (the sharp electrode of negative polarity) gain enough energy to remove two electrons from cathode's metal surface. Then one electron is ejected while the second neutralizes the ion. This process is known as secondary electron emission and its rate is defined by the Townsend's second ionization coefficient γ. Thus, secondary ionization provides additional electrons into ionization layer. These secondary electrons attach to neutral molecules outside the ionization layer, providing additional charge carriers and the total current increases. The secondary ionization coefficient is defined as the ratio of the production rate of secondary electrons to the rate of electron-impact ionization [9], is estimated to be of the order of 10^{-1} for a cathode's radius of curvature of 10^{-6}m [10]. This radius equals approximately to one of the needle tip. Thus, the increase of total negative current at pre-breakdown voltage of about 35%, with respect to positive one, is in good agreement with analytical [10] and experimental [11] results. The secondary ionization provides additional ions that result in $DeNO_x$ process improvement. The behavior of NO_x cleanness versus applied voltage, shown in Fig. 4 points at the significant advantage of negative corona over positive one.

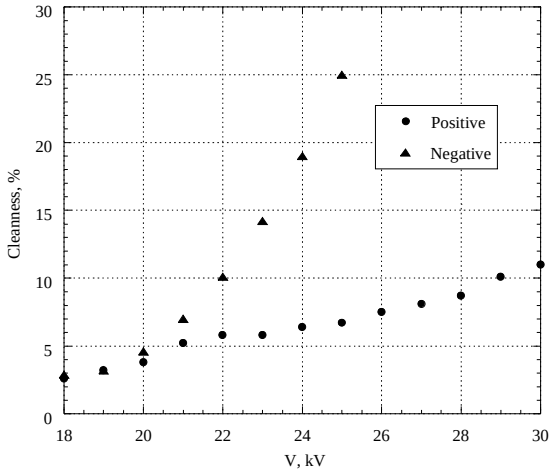

Fig.4: NO_x cleanness, *D*=30mm. *L*=50mm, *a*=10mm, load 2.5kW.

However, such an improvement of $DeNO_x$ process, when negative polarity is set on the needles, can not be explained by secondary ionization only. The additional improvement of cleanness follows from two reasons. The first is the presence of OH^- ions, produced from water molecules, in the drift region, which make significant contribution to NO_x removal. The presence of water in the reactor may improve the DeNOx process by several times [12]. The second reason is the production of chemically active radicals just outside the ionization layer. Electrons just beyond the ionization layer are still of sufficient energy and number in order to induce electron-impact reactions. Thus, plasma region, defined as a region in which corona enhanced dissociation chemical reactions are possible, extends beyond the ionization layer. Plasma boundary can be defined by electric field intensity of 16kV/cm [12]. At this value, the mean kinetic energy of electrons is 1.85eV and some electrons are energetic enough to participate in dissociation reaction. For instance, 5% of electrons in plasma region have a kinetic energy higher than the measured dissociation energy of O_2, which is 5.1eV [13].

Keeping in mind that besides the applied voltage, current must be known in order to calculate the electric power supplied to the reactor, *Corona Power* is introduced. The dependence of energy consumption on corona power is shown in Fig.5.

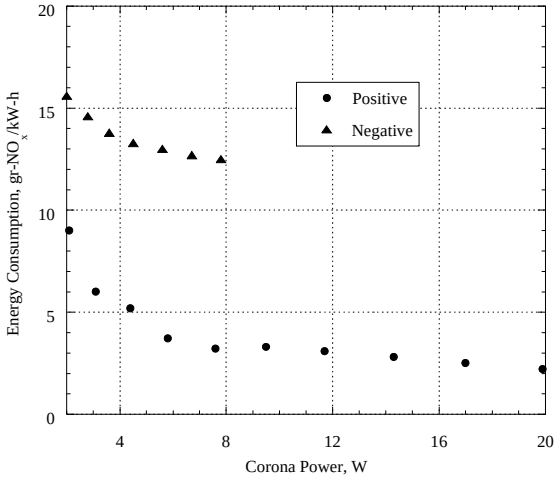

Fig.5: DeNO$_x$ energy consumption, D=30mm. L=50mm, a=10mm, load 2.5kW.

It can be seen from Fig.5 that energy consumption decreases with corona power growth. The energy consumption is calculated by:

$$Energy\ Consumption = \frac{Cleanness \times [NO_x]_{initial} \times Q \times \rho_{exhaust}}{Corona\ Power}$$

Where, Q is the flow rate, $[NO_x]_{initial}$ is the initial NO$_x$ concentration and $\rho_{exhaust}$ is the average density of exhaust gas. Since only the cleanness and the corona power vary with increase of voltage, while other parameters remain constant, the decrease in energy consumption is the result of insufficient rise of cleanness with non-linear increase of the applied power. When the applied voltage increases linearly, the growth of the total current appears to be faster than the increase of the cleanness, and therefore the energy consumption decreases.

From the experimental study of different engine loads it follows that cleanness is almost independent of the load applied, i.e. independent of the initial NO$_x$ concentration. The results of cleanness and energy consumption measurements are shown in Fig.6.

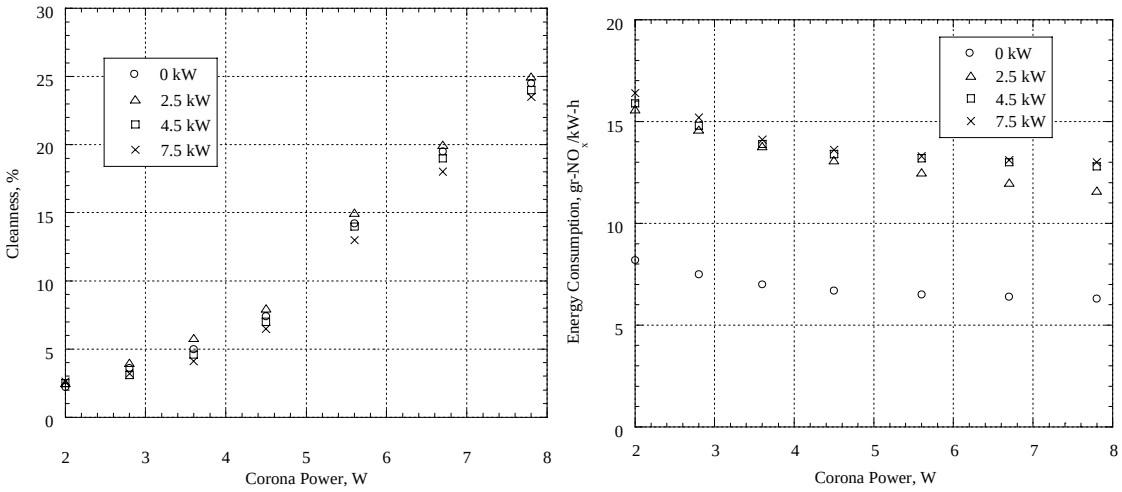

Fig.6: NO$_x$ cleanness and energy consumption for negative corona,

D=30mm. *L*=50mm, *a*=10mm.

Four typical values of engine loads were considered: 0kw, 2.5kW, 4.5kW, and 7.5kW, which provide initial NOx concentration of 300ppm, 560ppm, 600ppm, and 620ppm respectively. The independence of cleanness of initial NO_x concentration is possible only if the amount of the free electrons is significantly higher than the number of NO_x molecules in the exhaust gas. Since the energy consumption is derived from both corona power and cleanness, it is found to be relatively low for 0kW and twice as high for 2.5kW, 4.5kW, and 7.5kW. Observing the results, presented in Fig.6, the higher profitability of corona reactor for higher NO_x concentration is expected. Nevertheless, the NO_x concentration must not exceed the number density of the free electrons participating in the dissociation reactions.

The performance of the reactor is affected by both the electrode separation distance *D* and the number of installed needles *L*. For the purpose of estimating these effects, two independent sets of experiments were carried out: in the first one the number of installed needles *L* was kept constant while the distance *D* varied from 15mm to 50mm. In the second experiment, additional needles were installed (*L* increases) for the same distance *D*. The results are presented in the form of field diagram, shown in Fig.7. From this plot it follows that not only *D* and *L* affect the cleanness separately, but also their combination. The analysis of both longitudinal and altitudinal behavior of the cleanness is made, in order to provide physical explanation of the NO_x decomposition process.

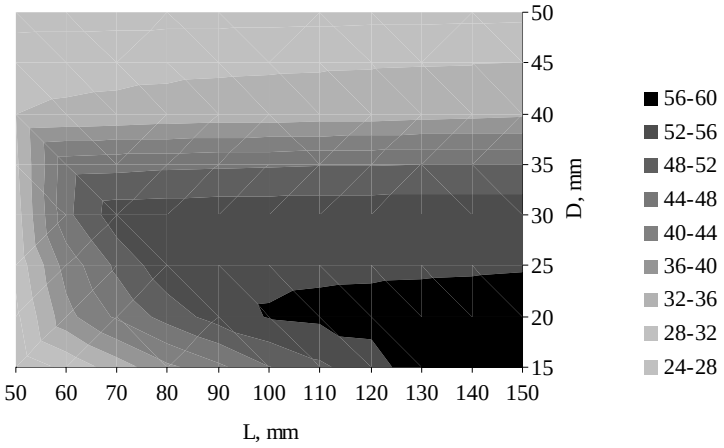

Fig.7: NO_x cleanness map for 2.5kW load, *a*=10mm.

The parameter that can characterize the effect of both *L* and *D* on NO_x removal rate is the time, which is spent by exhaust gas inside the discharge zone – *Residence Time* τ :

$$\tau = \frac{L \times D \times W}{Q}$$

Here, *W*=100mm is the reactor width, and *Q* is the exhaust gas flow rate. Basically, residence time defines the probability of interaction between the pollutant molecules and radicals produced by corona discharge. Keeping *L* constant and increasing *D* results in rise of cleanness initially due to increase of residence time, i.e. probability of NO_x chemical dissociation grows rapidly. Then, at some value of τ all the pollutant molecules interact with radicals and the cleanness reaches its maximum. Further increase of *D* causes the weakening of the electric field, which results in decrease of radicals' production, and therefore the cleanness decreases. When *D* is kept constant and *L* increases, the cleanness grows rapidly as a result of increase of residence time. Once the residence time is sufficient in order to all the

gas molecules interact with radicals, the cleanness growth rate attenuates. Further improvement of cleanness is much slower and demands a large amount of additional energy input. The value of cleanness, at which further $DeNO_x$ improvement almost stops, called *Asymptotic Cleanness*, and it lies between 50 and 60 percents. This low percentage follows from the fact that among radicals that react with pollutant, only O_2^- and OH^- decompose NO_x molecules [14], while the others do not participate in $DeNO_x$ process or even hinder it. Both tendencies of cleanness dependence on residence time are shown in Fig.8. It can be seen, that for a given *a*, the asymptotic cleanness is obtained at the same residence time, regardless of *D* and *L*. This value of τ provides optimal combination of *D* and *L*.

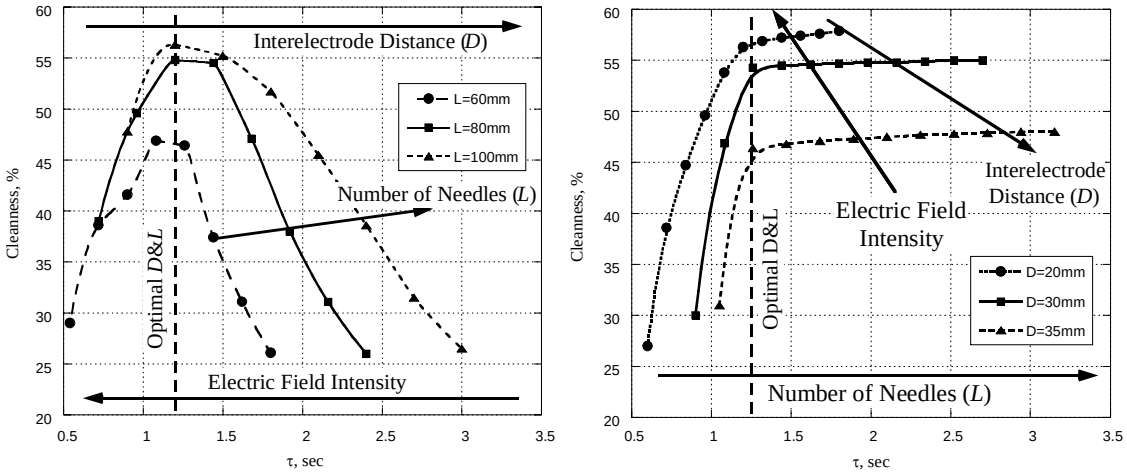

Fig.8: Cleanness VS residence time, *a*=10mm.

When the cleanness reaches its asymptotic value at a given *L* and *D*, the additional improvement of the reactor performance can be achieved by increasing the density of needles installation, i.e. decreasing of *a*. However, the smaller *a* results not only in production of extra radicals, but also in additional power input. This is similar to improvement of $DeNO_x$ process by the installation of additional needles (increase of *L*) for a given *a*, after the asymptotic cleanness is achieved. The residence time in this case is expected to be shorter relative to the one for larger *a*. The experiments show that the residence time, which corresponds to asymptotic cleanness, varies between 0.9 and 1.5 seconds, when *a* varies from 5 to 20mm respectively.

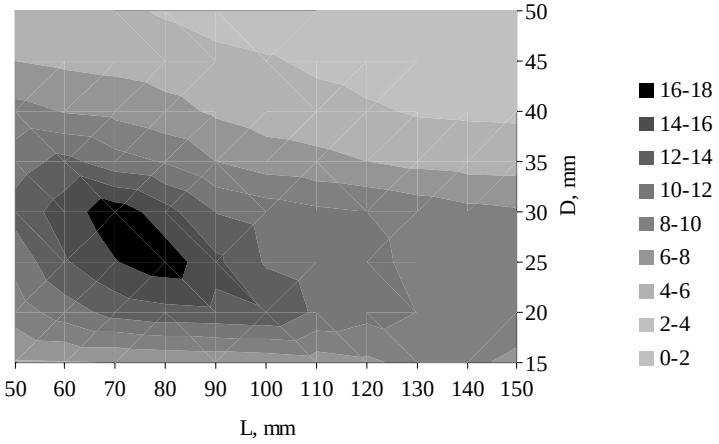

Fig.9: Energy consumption map for: *a*=10mm, 2.5kW load.

The cleanness optimization alone does not provide sufficient information for reactor design. The energy consumption must be considered as well, and then ultimately profitable combination of *D* and *L* can be obtained for each *a*, as it is shown in Fig.9. Summing up all the results, the plot that combines together the optimization of *L*, *a*, and *D*, which varies between 14 and 30mm is shown in Fig.10. When *D* is larger than 30mm the electric field is too low in order to sustain an effective NO_x removal, and hence is not worth using. The plot presents the cleanness behavior versus the corona power and refers to minimal *L*, i.e. *L* at which the asymptotic cleanness is obtained. As it is shown in Fig.10, the usage of smaller electrodes separation distance *D* is preferable for higher density of needles installation (smaller *a*), since with slight increase of power input the cleanness significantly increases. When *a* is between 15 and 20mm, the power consumed by the reactor at *D*=14mm is much higher than the one at *D*=30mm, and the increase in power input not compensated by improvement of $DeNO_x$ process.

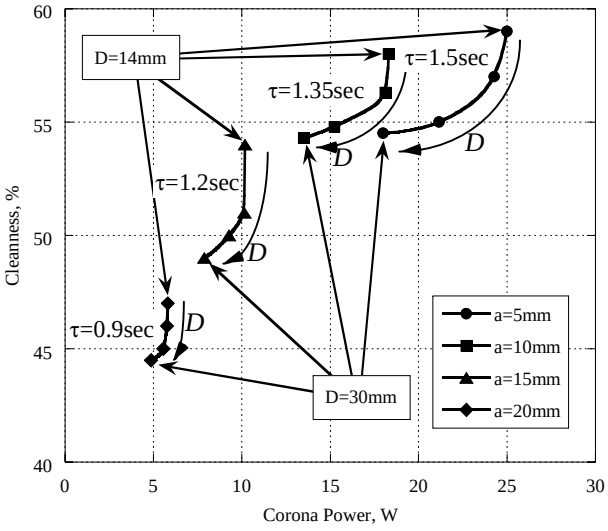

Fig.10: The cleanness behavior versus corona power.
(The intermediate points denote D=20mm and D=25mm)

The energy consumption for the points shown in Fig.10 varies between 15 and 30gr-NO_x/kW-h. These values are significantly higher than those obtained for DC corona with not optimized geometry [15]. The energy consumption of 30gr-NO_x/kW-h is of same order compared to the one obtained from the experiments with pulsed corona [16, 17]. Since the equipment required for pulsed corona reactor is expensive and technologically sophisticated, the DC corona reactor can be quite competitive.

1. E. Sher, *Handbook of Air pollution from Internal Combustion Engines*, Academic Press, 1998.
2. B. M. Penetrante, *Pollution Control Applications of Pulsed Power Technology*, Proc. of Ninth IEEE Int. Pulsed Corona Conf., 1-5, 1993.
3. S. Masuda, *Pulse Corona Induced Plasma Chemical Process - a Horizon of New Plasma Chemical Technologies*, Pure and Applied Chemistry, 60(5), 727-731, 1988.
4. J. A. Chalmers, *Atmospheric Electricity*, Clarendon Press, 1949.
5. J. J. Lowke, R. Morrow, *Theory of Electric Corona Including the Role of Plasma Chemistry*, Pure & Appl. Chem., 66(6), 1287-1294, 1994.
6. I. A. Kossyi, A. Y. Kostinsky, A. A. Matveyev, V. P. Silakkov, *Kinetic Scheme of the Nonequilibrium Discharge in Nitrogen-Oxygen Mixtures*, Plasma Sources Sci. Technol., 1(3), 207-220, 1992.
7. R. S. Sigmond, *Simple Approximate Treatment of Unipolar Space-Charge-Dominated Coronas: the Warburg Law and the Saturation Current*, J. Appl. Phys., vol. 53, No. 2, February 1982.
8. J. Vinogradov, E. Sher, I. Rutkevich, and M. Mond, *Voltage-Current Characteristics of a Flame-Assisted Unipolar Corona*, Combustion and Flame, 127, 2041-2050, 2001.
9. Y. P. Raizer, *Gas Discharge Physics*, Springer, New York, 1997.
10. J. Chen, J. H. Davidson, *Model of Negative DC Corona Plasma: Comparison to the Positive DC Corona Plasma*, Plasma Chem. And Plasma Proc., 23(1), (83-102), 2003.
11. A. Jaworek, A., Krupa, *Corona Discharge from a Multipoint Electrode in Flowing Air*, J. Electrostatics, 38, (187-197), 1996.
12. T. Fujii, Y., Aoki, N., Yoshioka, M., Rea, *Removal of NO_x by DC Corona Reactor with Water*, J. Electrostatics, 51-52, 8-14, 2001.
13. E. U. Condon, H. Odishaw, *Handbook of Physics*, McGraw-Hill, 1967.
14. D. J. Kim, Y. Choi, K. S. Kim, *Effects of Process Variables on NO_x Conversion by Pulsed Corona Discharge Process*, Plasma Chemistry and Plasma Processing, 21(4), 625-650, 2001.
15. H. Ohneda, A. Harano, M. Sadakata, T. Takarada, *Improvement of NO_x Removal Efficiency Using Atomization of Fine Droplets into Corona Discharge*, Journal of Electrostatics, 55, 321-332, 2001.
16. Y. S. Mok, S. W. Ham, I. S. Nam, *Evaluation of Energy Utilization Efficiencies for SO_2 and NO Removal by Pulsed Corona Discharge Process*, Plasma Chemistry and Plasma Processing, 18(4), 535-550, 1998.
17. E. M. van Veldhuizen, L. M. Zhou, W. R. Rutgers, *Combined Effects of Pulsed Discharge Removal of NO, SO2, and NH3 from Flue Gas*, Plasma Chemistry and Plasma Processing, 18(1), 91-111, 1998.